Inhibitory temporo-parietal effective connectivity is associated with explicit memory performance in older adults

Björn H. Schott[1,3,6,7], Joram Soch[1,2], Jasmin M. Kizilirmak[1], Hartmut Schütze[4,5], Anne Assmann[4,5], Anne Maass[4], Gabriel Ziegler[4,5], Magdalena Sauvage[3], and Anni Richter[3]

[1] German Center for Neurodegenerative Diseases (DZNE), Göttingen, Germany

[2] Bernstein Center for Computational Neuroscience (BCCN), Berlin, Germany

[3] Leibniz Institute for Neurobiology (LIN), Magdeburg, Germany

[4] German Center for Neurodegenerative Diseases (DZNE), Magdeburg, Germany

[5] Otto von Guericke University, Medical Faculty, Magdeburg, Germany

[6] Center for Behavioral Brain Sciences (CBBS), Magdeburg, Germany

[7] Department of Psychiatry and Psychotherapy, University Medical Center Göttingen, Göttingen, Germany

Address for correspondence:

PD Dr. Dr. Björn Hendrik Schott

Leibniz Institute for Neurobiology

Brenneckestr. 6

39118 Magdeburg, Germany

bschott@lin-magdeburg.de / bjoern-hendrik.schott@dzne.de

Key words: subsequent memory effect, episodic memory, dynamic causal modeling, fMRI, cognitive aging, precuneus, hippocampus

Abstract

Successful explicit memory encoding is associated with inferior temporal activations and medial parietal deactivations, which are attenuated in aging. Here we used Dynamic Causal Modeling (DCM) of functional magnetic resonance imaging data to elucidate the information flow between hippocampus, parahippocampal place area (PPA) and precuneus during encoding of novel visual scenes. In 117 young adults, DCM revealed pronounced activating input from the PPA to the hippocampus and inhibitory connectivity from the PPA to the precuneus during novelty processing, with both being further up-regulated during successful encoding. This pattern could be replicated in two cohorts (N = 141 and 148) of young and older adults. In both cohorts, older adults selectively exhibited attenuated (negative) PPA-precuneus connectivity, which correlated negatively with memory performance. Our results provide insight into network dynamics underlying explicit memory encoding and suggest that age-related differences in memory-related network activity manifest in altered temporo-parietal neocortical rather than hippocampal connectivity.

Outline

1. Introduction

One of the core questions in the cognitive neuroscience of episodic memory is why some experiences are encoded into stable memory traces that can subsequently be retrieved, while other experiences are forgotten. In functional magnetic resonance imaging (fMRI) studies of episodic memory, this question is commonly investigated using the so-called subsequent memory approach (Paller et al., 1987). Since its first application to fMRI (Brewer et al., 1998; Wagner et al., 1998), numerous studies have convergingly shown that successful encoding robustly engages the medial temporal lobe (MTL) and particularly the hippocampus (HC), as well as inferior temporo-occipital regions like the parahippocampal place area (PPA), prefrontal, and lateral parietal cortices (for a meta-analysis, see (Kim, 2011)). On the other hand, structures of the cortical midline like the precuneus (Prc) and the medial prefrontal cortex (mPFC), which form part of the Default Mode Network (DMN), are associated with relative deactivations during successful versus unsuccessful encoding (Kim, 2011; Maillet and Rajah, 2014).

Memory almost invariably declines with increasing age, and this decline is accompanied by characteristic alterations in memory-related network activations, including a reduced activation in inferior temporal cortices like the PPA and a reduced deactivation or even atypical activation of DMN, and particularly cortical midline structures such as the Prc ((Düzel et al., 2011; Morcom et al., 2003); for a review and meta-analysis, see (Maillet and Rajah, 2014)). Despite the robustness of these findings, the neural mechanisms underlying the relatively higher DMN activity during encoding still remain unclear. They may reflect increased reliance on DMN-dependent cognitive processes like self-referential or prior knowledge-dependent information during encoding (Maillet and Rajah, 2014) or a reduced ability to suppress unwanted DMN activity, reflecting lower processing efficiency or specificity (Grady et al., 2006; Hafkemeijer et al., 2012; Malagurski et al., 2020).

One potential mechanism mediating encoding-related hyperactivation of DMN structures in older adults could be increased excitatory or decreased inhibitory connectivity within the temporo-parietal memory network. The HC is highly interconnected with distributed neocortical regions (Deshpande et al., 2022), and previous studies have highlighted both the importance of hippocampal-neocortical connectivity for successful memory formation (Beason-Held et al., 2021; Cohen, 2011; Cooper and Ritchey, 2019; Fuentemilla et al., 2009; Schott et al., 2011; Schott et al., 2013) and the susceptibility of memory-related network connectivity to age-related alterations (Beason-Held et al., 2021; Stark et al., 2021).

Most functional connectivity measures, however, do not normally allow inferences about the directionality of information flow or about its excitatory versus inhibitory nature. Such information can be deduced from analyses of *effective* connectivity, such as Granger causality analysis (GCA) or Dynamic Causal Modeling (DCM) (Penny et al., 2004), but these approaches have thus far rarely been used in the context of memory encoding in older adults. Results from previous studies suggest that prefrontal-hippocampal effective connectivity becomes less task-specific in older adults with memory impairment (Nyberg et al., 2019) and that age-related deficits in HC-dependent navigation learning may be explained by higher HC excitability in older adults (Diersch et al., 2021). However, no studies have thus far characterized the encoding-related information flow between the HC and the brain structures that show the most prominent age-related under-recruitment (i.e., inferior temporal structures involved in stimulus processing, and particularly the PPA) and over-recruitment (i.e., DMN structures, and particularly the Prc), respectively.

In the present study, we used DCM on fMRI data acquired during a visual memory encoding paradigm, in which novel photographs of scenes were presented intermixed with familiar scenes and encoded incidentally via an indoor/outdoor decision task. Memory was tested 70 min later via an old/new recognition memory task with a five-step confidence rating (Düzel et al., 2011; Kizilirmak et al., 2022; Soch et al., 2021b) (Figure 1). Successful memory formation was associated with activation of the HC and the PPA as well as deactivation of the Prc in three independent cohorts (cohort 1: 117 young, cohort 2: 58 young, 83 older; cohort 3: 64 young, 84 older; see Table 1). In two cohorts that included both young and older adults, we could further replicate the previously reported age differences in memory encoding with older adults showing reduced activation of the PPA, but relatively increased activity in the Prc (Figure 2), while young and older adults showed comparable involvement of the anterior HC in successful encoding (Maillet and Rajah, 2014).

Based on these findings, we analyzed patterns of effective connectivity between the hippocampus and temporo-parietal memory network nodes, using the parametric empirical Bayes framework (Zeidman et al., 2019a; Zeidman et al., 2019b). We constructed a DCM model that included the HC, the PPA and the Prc as regions of interest (ROIs), exposure to novel stimuli as driving input to the PPA, and successful memory formation as a potential parametric modulator at each connection between the three ROIs (Figure 1). The PPA is thought to process and analyze the novel scene, binding its elements and incorporating the current context, which is then bound and encoded together by the HC (Aminoff et al., 2013). Therefore, we first hypothesized that successful encoding would be associated with an up-regulation of

information flow from the PPA to the HC. The precuneus constitutes a core structure of a parietal memory network (PMN) proposed by Gilmore, Nelson and McDermott (Gilmore et al., 2015). The PMN has been associated with higher responses to familiar compared to novel stimuli and with negative subsequent memory effects (or "subsequent forgetting effects") in young adults (Uncapher and Wagner, 2009), which are attenuated or even inverted in older adults (Maillet and Rajah, 2014). Based on those observations, we further hypothesized that successful memory formation would be associated with a down-regulation of information flow (i.e., more pronounced inhibitory effective connectivity) to the Prc from either the PPA or the HC. With respect to age effects, we further hypothesized that at least one of the aforementioned mechanisms – i.e., enhanced information flow to the hippocampus and inhibitory effective connectivity to the precuneus - would be attenuated in older adults, which in turn would be associated with poorer memory performance within the group of older adults. To this end, we performed correlational analyses between connection strength and memory performance (area under the curve, A'; (Soch et al., 2021a)).

2. Results

In the three independent cohorts, a characteristic pattern of novelty-related effective connectivity and encoding-related modulation could be identified. In cohorts 2 and 3, we could further observe age-related reductions in PPA-Prc effective connectivity that correlated with memory performance in the older participants.

2.1.Activations and deactivations during memory encoding in young and older adults

Figure 2 displays representative activations and deactivations during successful memory encoding (parametric memory regressor). Using voxel-wise one-sample t-tests performed in SPM12, we could replicate previously reported encoding-related activations and deactivations (Kim, 2011) in cohort 1. Successful episodic memory encoding was associated with increased activation of the HC and an extensive temporal and inferior parietal network, including a pronounced local maximum in the PPA (Figure 2, left column). In cohorts 2 and 3, we additionally tested the age-related activation differences during successful encoding (Figure 2, middle and right column). Replicating previous studies (Maillet and Rajah, 2014), we found older participants to exhibit lower activations in inferior and medial temporal structures, including the PPA, but relatively preserved encoding-related activation of the HC. Furthermore, in line with earlier studies, older adults exhibited reduced deactivations in midline structures of the DMN during successful encoding, with the maximum between-group difference in the right Prc.

2.2.Temporo-parietal effective connectivity and its modulation during memory encoding

Figure 3A displays the intrinsic connectivity of the temporo-parietal network (A-matrix) during novelty processing investigated in our DCM analyses, separated by main effects (top row) and age differences (bottom row). Connectivity changes related to successful memory formation (B-matrix) are displayed in Figure 3B, following the same layout as Figure 3A. Posterior connection strengths are displayed in Figure 4, highlighting connections that could be replicated across all three cohorts (or across cohorts 2 and 3 in case of age group effects).

Intrinsic connectivity between regions: Across all cohorts, there were pronounced excitatory connections from the PPA to the HC and from the HC to the Prc (Figure 3A, top row). A pronounced inhibitory connection was observed from the PPA to the Prc. All of these connections reached a posterior probability (PP) of 1.00 in all three cohorts (see also Figure 4, left panels) and were significantly different from 0 at $p < .05$, FDR-corrected. In cohorts 1 and 2, a positive connection was evident from the Prc to the PPA. In cohort 3, this connection

reached a PP of > .95 in older adults only, albeit being significantly different from 0 in the entire cohort.

Intrinsic inhibitory self-connectivity: In the DCM framework, self-connectivity is *a priori* expected to be inhibitory, with higher negative values reflecting stronger (self-)inhibition (Yang et al., 2017). Self-connectivity is reflected in the diagonals of the matrices in Figure 3A (top row). Across all three cohorts, we observed negative self-connectivity of the HC (Figure 3A, top row; Figure 4, left panels), most likely reflecting reduced auto-inhibition (relative to the implicit baseline) during processing of the novel stimuli, which served as driving input. No clear pattern emerged with respect to self-connectivity of the PPA or the Prc.

Memory-related connectivity changes (contextual modulations): Successful encoding, as captured by the parametrically modulated memory regressor was associated with increased effective connectivity from the PPA to the HC and more pronounced negative effective connectivity from the PPA to the Prc (Figure 3B, top row). These connectivity changes could be replicated in all three cohorts (Figure 4, left panels, red bars). Additionally, in cohort 1, we observed increased bidirectional encoding-related effective connectivity between the HC and the Prc, but, in cohorts 2 and 3, these parameters did not exceed the *a priori* defined threshold of PP > .95.

2.3.Age-related difference in memory network effective connectivity

As there were no older adults in cohort 1, all age differences reported here are based on cohorts 2 and 3. In both cohorts, age group was associated with more positive (i.e., reduced inhibitory) effective connectivity from the PPA to the Prc (Figure 3A/B, bottom rows; Figure 4, right). This reduced inhibitory temporo-parietal effective connectivity was found in the A-matrix (intrinsic connection) in both cohorts, and, additionally, in cohort 3, it was also found in the B-matrix (memory-related contextual modulations). Furthermore, even though there was no clear age-independent pattern (see 3.2) of Prc self-connectvity across the three cohorts, inhibitory Prc self-connectivity was nevertheless reduced in older adults compared to young adults in both cohorts 2 and 3.

2.4.Association between PPA-Prc inhibitory effective connectivity and memory performance in older adults

As described above, the inhibitory connection from the PPA to the Prc was attenuated in older compared to young adults (Figure 3A, bottom row; Figure 4, right panels). We therefore focused on this connection when testing for a relationship between DCM parameters and

memory performance in older adults. In both cohorts (2 and 3), the parameter representing PPA-Prc connectivity was negatively correlated with A' as measure of memory performance (cohort 2: $\Pi = -0.37$, $p = .0022$; cohort 3: $\Pi = -0.30$, $p = .0185$; outlier-robust Shepherd's Pi correlations; Figure 5A), such that stronger PPA-Prc inhibitory connectivity related to better memory performance. When computing exploratory Pearson's correlation coefficients for A' and all DCM parameters, we found that only the correlation with the PPA-Prc connection was significant in both cohorts (surviving FDR correction in cohort 2; Figure 5B).

3. Discussion

In the present study, we have employed DCM to elucidate the putative temporo-parietal information flow underlying fMRI activations and deactivations during successful memory formation and their characteristic age-related differences. We found that successful memory encoding was associated with increased PPA-hippocampal effective connectivity and increased inhibitory effective connectivity from the PPA to the Prc in both young and older adults. In older adults, the inhibitory connection from PPA to Prc was, however, reduced, and less negative inhibitory – or even positive – PPA-Prc connectivity was associated with poorer memory performance.

3.1.Cortical-hippocampal interactions during novelty processing and memory encoding

In three independent cohorts, a characteristic pattern of intrinsic effective connections emerged, which were in part further modulated as a function of encoding success (for an overview, see Figure 6). Most prominently, the following connections were observed:

1. *The PPA exerts novelty-related excitatory input on the HC, which is up-regulated during successful encoding*. Previous studies have demonstrated that both the HC and the PPA exhibit robust responses to novel scenes (Köhler et al., 2002; Kremers et al., 2014) as well as subsequent memory effects (Dennis et al., 2008; Soch et al., 2021a). The direction of information flow from the PPA to the HC observed in the present study suggests that HC-dependent encoding of the stimuli occurs *after* higher-level perceptual analysis of the scene stimuli in the PPA. This interpretation is supported by previous neuroimaging studies (Aminoff et al., 2013; Eichenbaum et al., 2007) as well as by electrophysiological investigations and immediate-early gene imaging studies in rodents, which, despite the lack of a clearly defined homologue of the PPA in rodents, support the notion that scene processing is mediated by the parahippocampal cortex (Kinnavane et al., 2014) and that hippocampal encoding of episodes is preceded by stimulus processing in inferior-medial temporal cortices (Marks et al., 2021; Olarte-Sánchez et al., 2014).
2. *The HC shows negative self-connectivity during novelty processing.* Self-connections are an integral part of any functional network, because they control the excitatory-inhibitory balance (Snyder et al., 2021). Self-connectivity is *a priori* defined as negative within the DCM framework (Yang et al., 2017), and a negative value of self-connectivity would thus reflect release of self-inhibition of the HC. As the "baseline" connectivity patterns reported in our study are in fact the connectivity patterns upon driving input (here: activation of the

PPA in response to novel scene stimuli) (Epstein and Baker, 2019), we suggest that the negative self-connectivity of the HC found in our DCM analysis most likely reflects hippocampal novelty responses to the previously unseen scene stimuli. The HC exhibits strong responses to novel stimuli (Kumaran and Maguire, 2007; Ranganath and Rainer, 2003), a finding also replicated in another cohort of older adults using the same paradigm as in the present study (Billette et al., 2022; Düzel et al., 2022).

3. *The PPA exerts inhibitory input to the Prc during novelty processing and successful encoding.* Deactivations of the Prc are a common finding in studies employing the subsequent memory effect (Kim, 2011; Uncapher and Wagner, 2009), and a straightforward explanation for this is that the Prc as a DMN structure deactivates during most tasks that require externally directed attention (Buckner et al., 2008), including novelty processing (Billette et al., 2022) and successful encoding (Kizilirmak et al., 2022; Maillet and Rajah, 2014). During encoding of novel stimuli, it may be of particular importance to suppress processing related to retrieval and familiarity, which engages the Prc (Gilmore et al., 2015; Kim, 2011; Qin et al., 2012). While the function of the Prc in explicit memory processes likely goes beyond supporting retrieval (see 4.2), it is notable from the present results that suppression of Prc activity during novel stimulus processing and successful encoding was not found to be mediated by the HC, but rather directly by the PPA, bypassing the HC.
4. *The HC exerts excitatory input to the Prc during novelty processing.* Unlike the PPA, the HC exerted positive input to the Prc during processing of novel stimuli, although there was only very limited evidence for a further modulation by encoding success (Figure 3, 4). One explanation for this may be that the hippocampal novelty signal is relayed to the Prc, allowing for novelty-related deactivation (Gilmore et al., 2015) (Section 4.2).
5. *The Prc exhibits positive effective connectivity to the PPA during novelty processing.* In cohorts 1 and 2 and in the older participants from cohort 3, we further found an excitatory connection from the Prc to the PPA. The Prc is strongly interconnected with the parahippocampal cortex (Ranganath and Ritchey, 2012), of which the PPA is a subregion. Projections from the Prc to the parahippocampal cortex are thought to be of a feed-backward type. One possible function of this connection could be that the Prc provides information based on existing knowledge that can be used to integrate elements of a novel scene into existing memory representations (for a detailed discussion, see 4.2).

3.2.The multifaceted role of the precuneus in human long-term memory

The engagement of DMN structures during memory retrieval processes is a well-replicated finding (Buckner et al., 2008; Qin et al., 2012), and the Prc, in particular, is well-known for its role in episodic retrieval (Kim, 2011), despite an ongoing debate with respect to a preferential role in recollection versus familiarity (Gilmore et al., 2015; Vilberg and Rugg, 2008). Irrespective of the type of retrieval process involved, it seems plausible to assume that, during processing of novel stimuli, suppressing Prc activity may help to reduce interference with familiar information. In line with this interpretation, Gilmore and colleagues proposed a parietal memory network that includes the Prc, which deactivates in response to novel information and shows increased responses as a function of stimulus familiarity (Gilmore et al., 2015).

During successful encoding, higher activity in ventral parietal structures has been associated with subsequent forgetting rather than remembering (Gilmore et al., 2015; Kim, 2011; Uncapher and Wagner, 2009). On the other hand, there has also been evidence for higher activity in dorsal parietal structures associated with positive subsequent memory effects (Uncapher and Wagner, 2009). While the meta-analysis by Uncapher and Wagner was focused on lateral parietal structures, a similar pattern of functional heterogeneity has also been proposed for midline parietal subregions of the DMN (Kernbach et al., 2018). Particularly the dorsal Prc is involved in switching between DMN activity and activity of task-positive networks (Utevsky et al., 2014) and has been shown to be actively engaged in some attention-demanding tasks, possibly mediating the integration of inwardly-directed and externally-directed cognitive processes (Lyu et al., 2021). More recently, the precuneus has also been proposed as a key region for memory acquisition (Brodt et al., 2018; Brodt et al., 2016; Schott et al., 2019). However, those studies all employed repeated stimulus exposure, and may therefore reflect a primarily neocortically-mediated form of learning distinct from hippocampus-dependent memory for unique episodes (Henke, 2010).

One possibility to reconcile those findings with the results of our present study is that the Prc may serve, to some extent, as a gatekeeper during long-term memory formation, enabling the parallel storage of unique episodes in their spatial and temporal context and of elaborate and multiply associated information (i.e., schemas) (Henke, 2010; van Kesteren et al., 2012). More broadly, future research should explore the possibility that parietal memory network structures may contribute to the distinction of episodic and semantic memory (Renoult et al., 2019).

3.3.Neocortical inhibitory connectivity and memory performance in older adults

While both reduced MTL gray matter volumes and lower episodic memory performance in older adults are well-replicated findings (Nyberg, 2017), our present study yielded no evidence

for a relationship between hippocampal effective connectivity and memory performance in the older participants. Instead, among all DCM parameters tested, only the inhibitory connection from the PPA to the Prc was associated with memory performance in older adults. Specifically, a better-preserved inhibitory input from the PPA to Prc during encoding of novel stimuli correlated with better performance in the subsequent memory test (Figure 5). We therefore tentatively suggest that the commonly observed decreased encoding-related DMN deactivation in older adults – and especially in those with poor memory performance – (Maillet and Rajah, 2014) may result from a reduced ability to suppress ongoing DMN activity. This interpretation may be somewhat at odds with the commonly proposed notion that increased activation of parietal – and also prefrontal – neocortical structures may reflect a compensatory mechanism for diminished MTL function in old age (Cabeza et al., 2018; Maillet and Rajah, 2014).

One possible interpretation for this apparent discrepancy is that compensatory activity might be particularly relevant in older adults with pre-clinical or subclinical memory impairment. While preserved patterns of memory-related brain activity (i.e., patterns with high similarity to those of young adults) have been associated with better memory performance in older adults (Düzel et al., 2011; Richter et al., 2022; Soch et al., 2022; Soch et al., 2021a), those with poorer memory performance can show not only deactivations, but even atypical activations of DMN structures during successful versus unsuccessful encoding (Maillet and Rajah, 2014), possibly reflecting an increased reliance on self-referential or prior knowledge-dependent information during encoding (Chen et al., 2022; Kizilirmak et al., 2021; Li et al., 2022).

Increased activity of midline brain structures during novelty processing and successful memory encoding has been reported in individuals at risk for Alzheimer's disease (AD), that is, otherwise healthy older adults with subjective cognitive decline (Billette et al., 2022) or cognitively unimpaired older individuals with increased beta-amyloid deposition as assessed with PET (Sperling et al., 2009). Notably, this DMN hyperactivation is no longer observed in patients with early-stage AD (Billette et al., 2022). Whether this pattern reflects compensatory mechanisms at a pre-clinical stage that break down during disease progression or rather a more general impairment of inhibitory processes that precedes a broader decline in neural function is yet unclear. More recent data (Vockert et al., in preparation[1]) suggest that preserved encoding-related DMN deactivations in individuals with amyloid or tau pathology are associated with better cognitive performance, thus supporting the latter interpretation.

[1] The manuscript by Vockert et al., is to be submitted in due course and will be cited fully in the final version of this manuscript.

Age-related increases activations of brain activity not typically involved in a task have also been observed in cognitive domains other than explicit memory (Sambataro et al., 2010), and even in the motor system (Knights et al., 2021). As, in the latter study, ipsilateral motor system activity did not predict better performance (e.g., reaction times), the authors suggested that their results speak against a compensatory role of age-related task-related hyperactivations. Together with our present results, we suggest that loss of inhibitory activity might constitute a cross-domain mechanism of brain aging, and future research should further explore its possible relationship with subclinical pathology.

3.4.Limitations and directions for future research

A limitation of the present study is inherent to the DCM approach, that is, the restriction to the *a priori* selected regions included in the model (Lohmann et al., 2012). In the present study, we defined our ROIs based on anatomical constraints, literature-based assumptions, and group activations, and further restricted them based on individual subjects' first level contrasts, to improve signal-to-noise ratio (see Methods, 2.6.1). This rather rigid approach may limit the comparability to previous DCM studies. Furthermore, our model did not include prefrontal cortex regions, which are typically involved in successful episodic encoding (Kim, 2011). In a DCM study of hippocampal-prefrontal effective connectivity during memory formation in older adults, Nyberg and colleagues showed that higher prefrontal-hippocampal connectivity during encoding was associated with higher dropout rate from a longitudinal study, as a proxy for worse cognitive and clinical outcome (Nyberg et al., 2019). Along the same line, we did not assume a modulation of self-connectivity in our model space, as we had no plausible hypotheses regarding their modulation. One study on hippocampal-posterior neocortical effective connectivity during spatial navigation suggested that reduced hippocampal auto-inhibition was associated with lower learning performance in older adults (Diersch et al., 2021). While, unlike in those studies, we did not observe age-related changes in hippocampal effective connectivity in our present DCM study – most likely due to differences in the underlying models –, we nevertheless suggest that the reduced neocortical inhibitory connectivity found here converges with the aforementioned results in highlighting the role of inhibitory connectivity within the temporo-parietal memory networks in successful aging of human memory systems.

Beyond ROI selection, it must be noted that the DCM approach relies on multiple highly complex assumptions with respect to functional neuroanatomy (see above), model space and model selection (Daunizeau et al., 2011; Lohmann et al., 2012), but also the underlying biophysical mechanisms when inferring on a neuronal state from a hemodynamic signal

(Daunizeau et al., 2011). It is thus likely overstated to assume direct causality from the effective connectivity patterns observed, and we are aware that our model, its reproducibility aside, is most likely incomplete.

Another limitation of the present study may result from the sampling of the study cohort (Soch et al., 2021a) and the lack of AD-related biomarkers. Despite the considerable interindividual variability in memory performance among the older adults in our cohort ((Kizilirmak et al., 2022), Figure 2), it must be acknowledged that older participants were most likely healthier than average. This was both due to our participant recruitment strategy, which led to healthy and active older adults to more likely volunteer for participation (see Methods, 2.1), and due to the exclusion of participants with severe comorbidity (Soch et al., 2021a). In a large cohort that included older adults with subjective cognitive decline (SCD) and mild cognitive impairment (MCI) as well as manifest AD, novelty-related Prc responses were found to exhibit an inverse U-shaped pattern from healthy older adults over SCD and MCI to manifest AD (Billette et al., 2022). It remains thus to be determined whether the association between temporo-parietal inhibitory connectivity and memory performance also applies to individuals with memory impairment or dementia risk states.

3.5.Conclusions

Using dynamic causal modeling on fMRI data acquired during a visual memory encoding task, we could demonstrate that successful memory formation is associated with increased information flow from the PPA to the hippocampus and suppression of information flow from the PPA to the precuneus. A preserved inhibitory PPA-precuneus connection was associated with better memory performance in two cohorts of healthy older adults. Our results highlight the importance of inhibitory mechanisms in successful aging of the human memory system. Future studies should investigate the longitudinal trajectories of inhibitory processes in human explicit memory, in order to explore the possibility that impaired inhibition might constitute an early pathophysiological mechanism in the development of age-related cognitive decline.

4. Notes

4.1. Acknowledgments

The authors would like to thank Nadia Ay, Hannah Feldhoff, Larissa Fischer, Sophia Jauch, Matthias Raschick, Marc Roder, and Annika Schult for help with neuropsychological data collection and analysis and Kerstin Möhring, Katja Neumann, Ilona Wiedenhöft, and Claus Tempelmann for assistance with MRI data acquisition. We further thank Emrah Düzel for helpful discussion during the planning stage and collaboration during data collection.

This study was supported by the State of Saxony-Anhalt and the European Regional Development Fund (Research Alliance "Autonomy in Old Age" to B.H.S.) and by the Deutsche Forschungsgemeinschaft (SFB 1436, TP A05 to B.H.S., TP B01 to M.S., TP C01 to G.Z., and TP Z03 to A.M.; DFG RI 2964-1 to A.R.). The funding agencies had no role in the design or analysis of the study. The authors have no conflict of interest, financial or otherwise, to declare.

4.2. Data Availability Statement

Due to data protection regulations, sharing of the entire data set underlying this study in a public repository is not possible. Access to de-identified raw data, Matlab scripts and ROIs used for data analysis will be provided by the authors upon reasonable request.

5. Tables

Table 1. *Demograhic and behavioral data, MRI acquisition parameters.*

	Cohort 1	Cohort 2	Cohort 3
Demographics			
young			
N	117	58	64
age	**24.37** (± 2.60)	**23.62** (± 3.45)	**24.45** (± 4.46)
gender (f/m)	57 / 60	28 / 30	37 / 27
older			
N	–	83	84
age	–	**65.20** (± 6.71)	**62.96** (± 6.06)
gender (f/m)	–	48 / 35	52 / 32
MRI parameters			
MRI scanner	Siemens Verio	Siemens Verio	Siemens Skyra
number of slices	40	47	47
TR / TE / flip-α	2.40 s / 30 ms / 80°	2.58 s / 30 ms / 80°	2.58 s / 30 ms / 80°
voxel size	2 x 2 x 3 mm	3.5 x 3.5 x 3.5 mm	3.5 x 3.5 x 3.5 mm
scanning time	494.4 s	531.5 s	531.5 s
unwarping	no	yes	yes
Memory performance			
young A’	**.81** +/- .075	**.83** +/- .073	**.82** +/- .068
older A’	n/a	**.78** +/- .072	**.77** +/- .077

Data are shown separately for each cohort. Abbreviations: N = sample size, f = female, m = male, TR = repetition time, TE = echo time, flip-α = flip angle; A’ = area under the curve in a ROC analysis of the recognition memory test, reflecting behavioral accuracy (hits vs. false alarms).

6. Figures

Figure 1. *Experimental paradigm and design of the DCM study.* During fMRI scanning, participants underwent an incidental visual memory paradigm. We used the novelty response to all novel pictures as driving input to the PPA and generated a parametric memory regressor by parametrically modulating the novelty response with the arcsine-transformed response in the delayed recognition task. The thus obtained memory regressor served as potential contextual modulator of the connections between the PPA, the hippocampus (HC) and the precuneus (Prc).

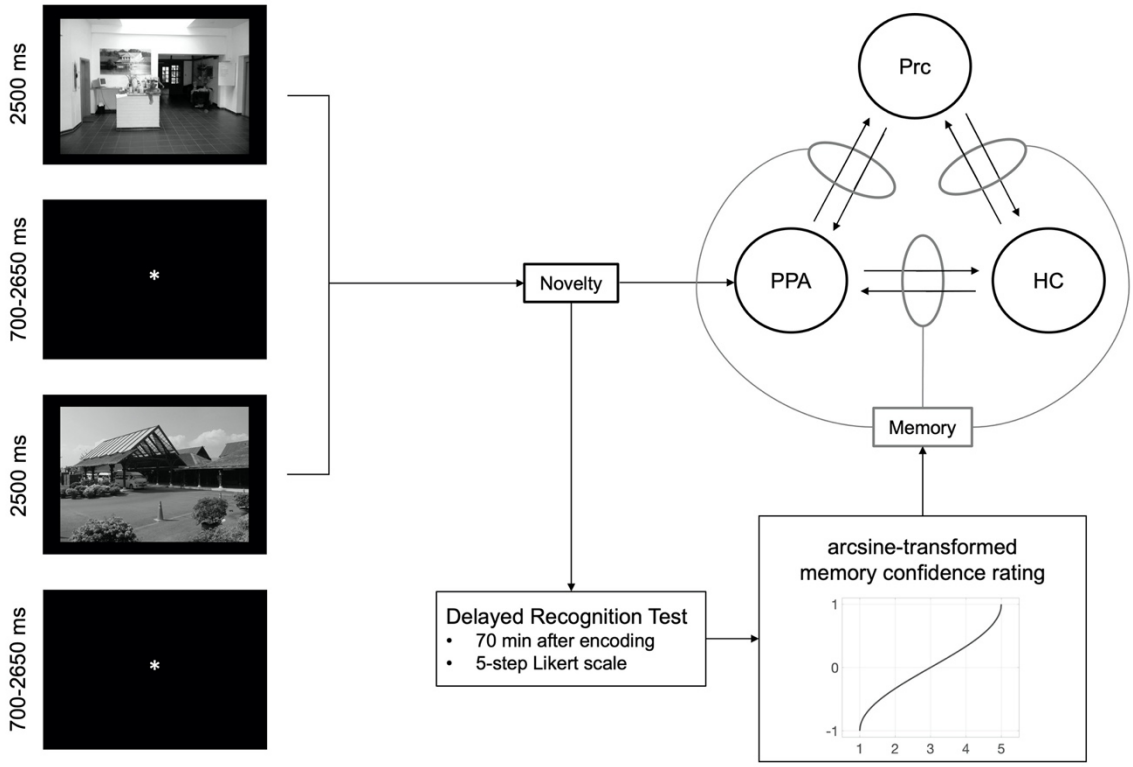

Figure 2. *Encoding-related activations and deactivations and their age-related differences.* Top row: In all three cohorts, successful episodic memory formation was associated with increased activation of the bilateral hippocampus (right hippocampus shown here). Middle row: Successful encoding also elicited activation of the PPA (left column) which was reduced in older relative to young adults (middle and right column). Bottom row: Encoding-related deactivations in the precuneus (left column) were reduced in older adults (middle and right column). All contrasts are displayed at $p < .05$, corrected for family-wise error (FWE) at voxel-level, with a minimum cluster size of $k = 10$ adjacent voxels. Coordinates denote local maxima of activation or activation difference in the respective contrasts.

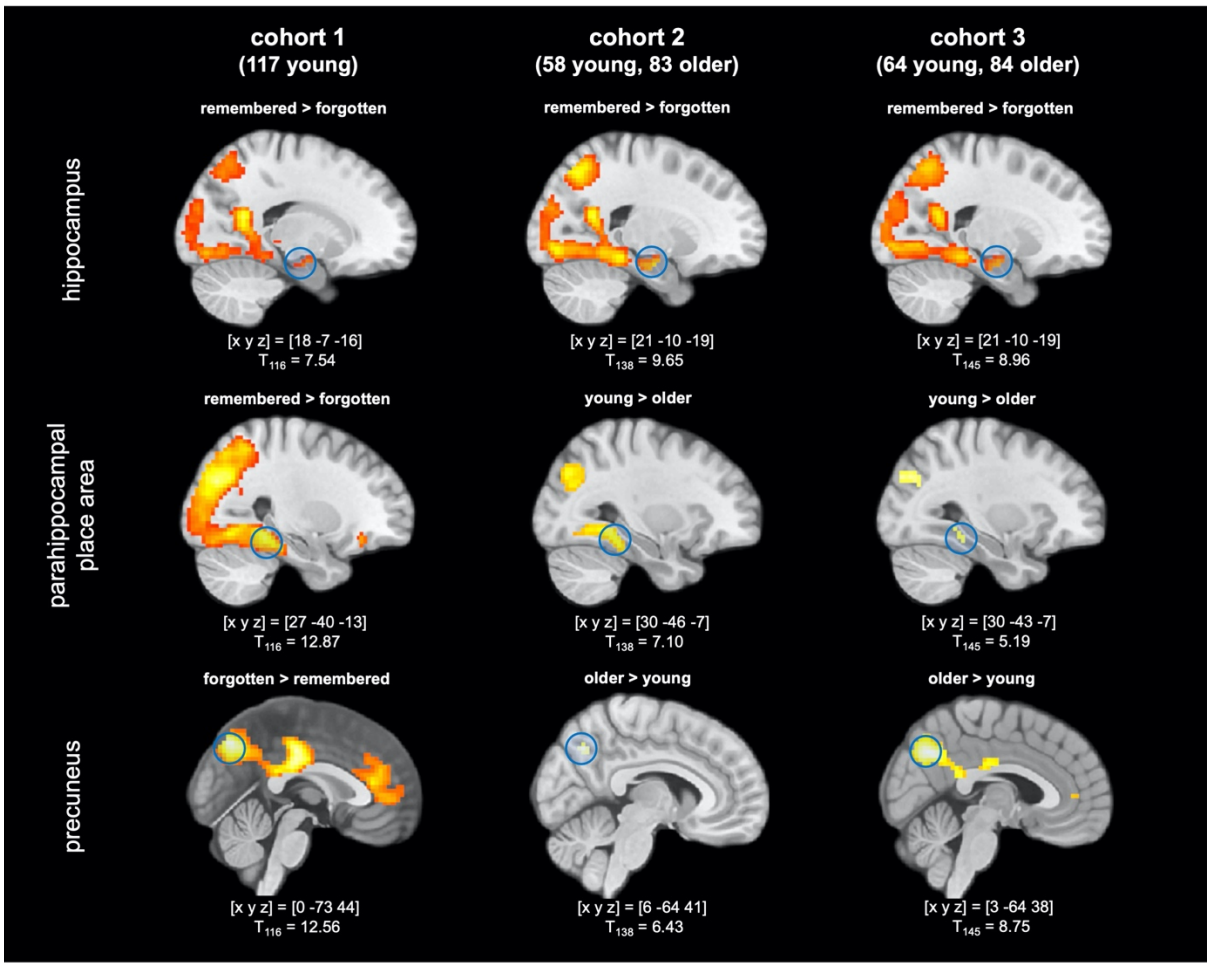

Figure 3. *Connectivity matrices of effective connectivity strengths and their modulation by age group.* **(A)** Intrinsic connections and **(B)** contextual modulations. Color denotes the parameter size, reflecting positive ("excitatory") vs. negative ("inhibitory" connectivity for main effects and higher vs. lower values in older adults for age effects. The posterior probability (PP) of a parameter being > 0 in absolute value are shown. Connections with PP < .95 are gray-shaded. Asterisks denote significance of classical test statistics. ** p < .05, FDR-corrected; * p < .05, uncorrected; (*) p < .10.

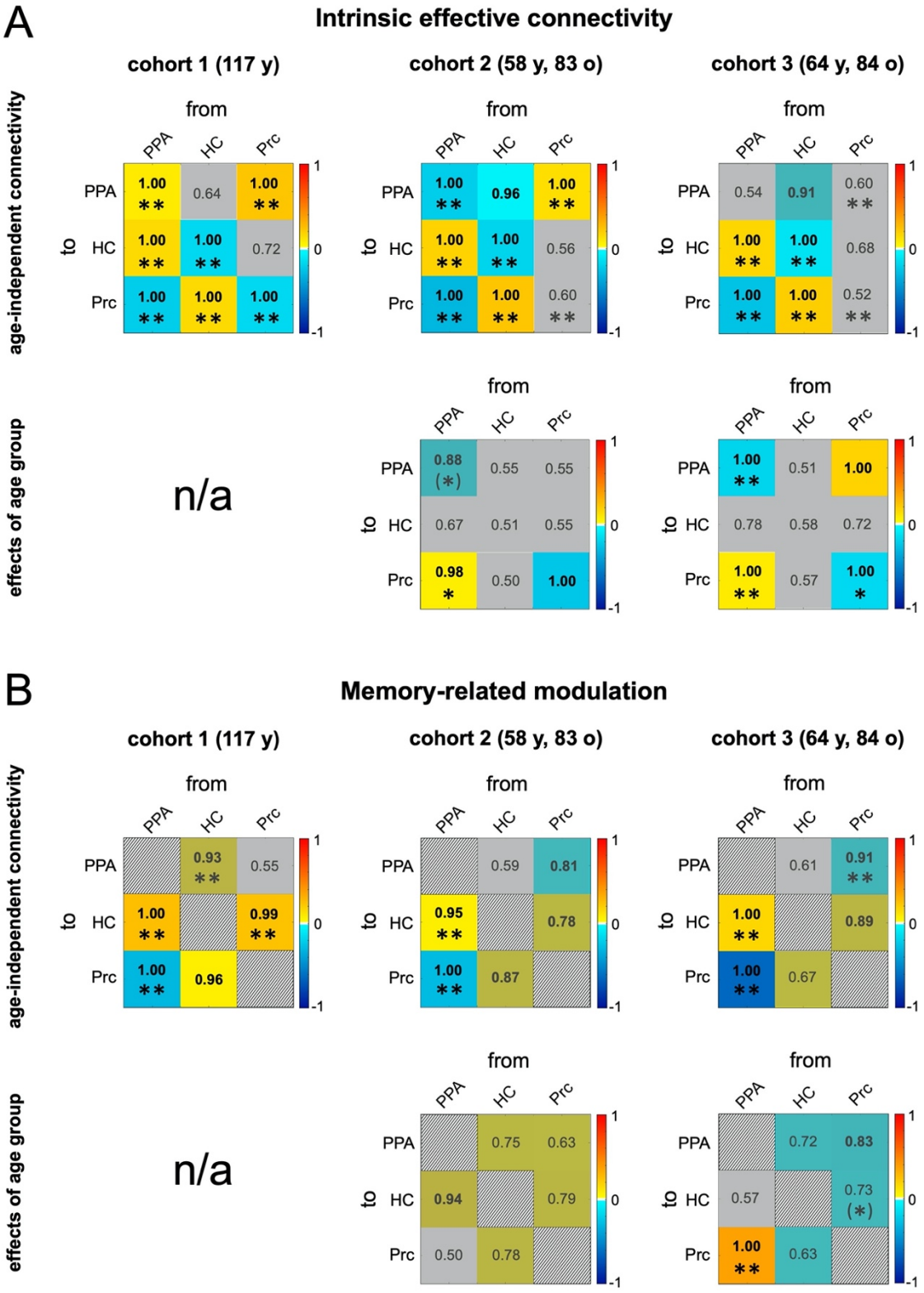

Figure 4. *Replicability of DCM results across cohorts.* Bar plots show group-level Bayesian mean parameter estimates and 90% confidence intervals. Grey bars denote intrinsic connections (A-parameters) and red bars denote contextual modulations (B-parameters). Plots highlighted in blue show connections that were replicated across all three cohorts (main effects, left panel) and in cohorts 2 and 3 (age group effects, i.e. older - young, right panel), respectively.

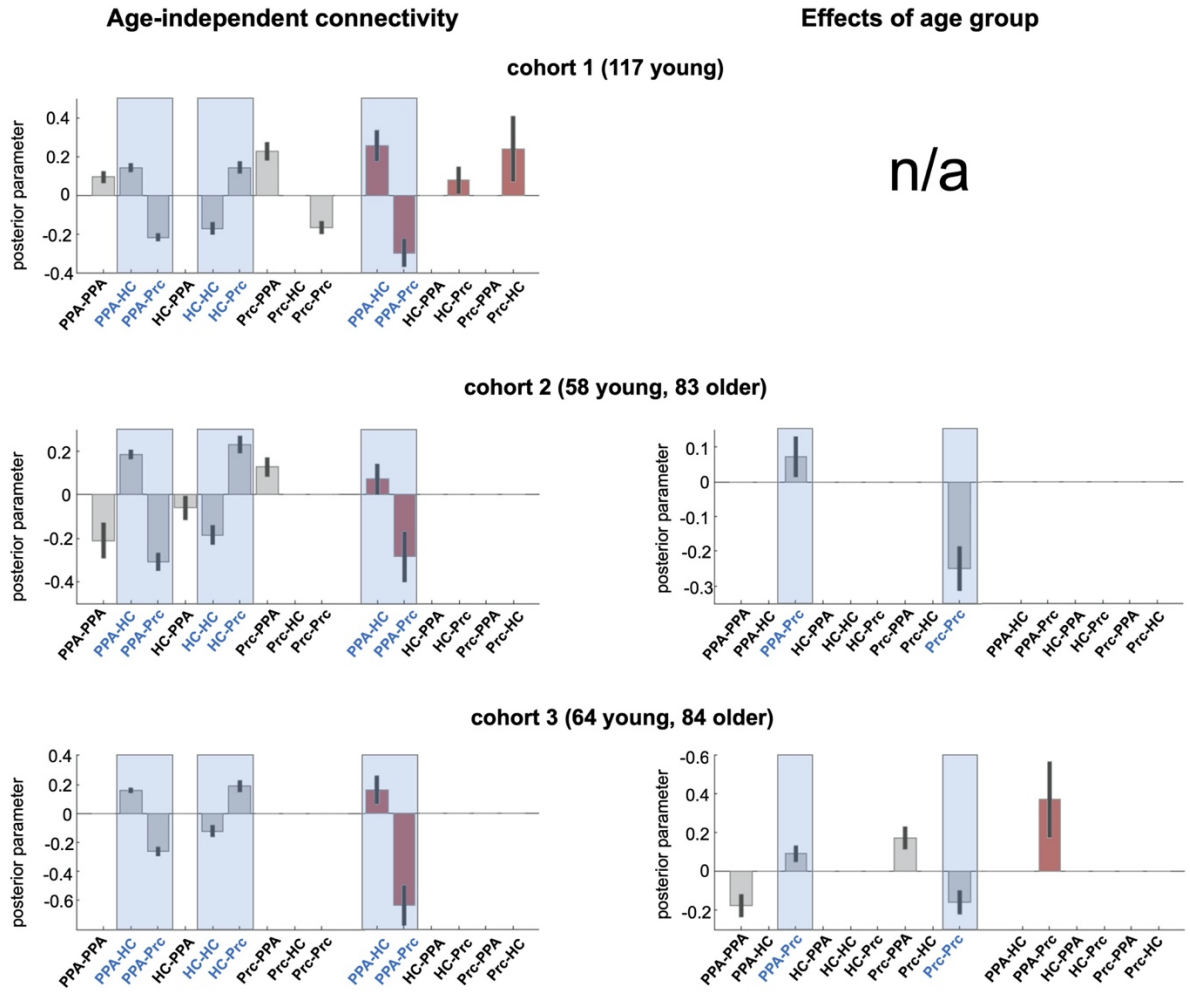

Figure 5. *Correlations between DCM parameters and memory performance in older adults.* **(A)** When computing outlier-robust Shepherd's Pi correlations, the correlation between the inhibitory PPA-Prc connection was significant in both cohorts. **(B)** Results from pair-wise Pearson's correlations of the individual participants' DCM parameters with memory performance (A'). Only the negative correlation with the inhibitory connection from the PPA to the precuneus in the A-matrix could be replicated in both cohorts 2 and 3. Positive and negative correlations are shown in red and blue, respectively. ** p < .05, FDR-corrected; * p < .05, uncorrected; (*) p < .10.

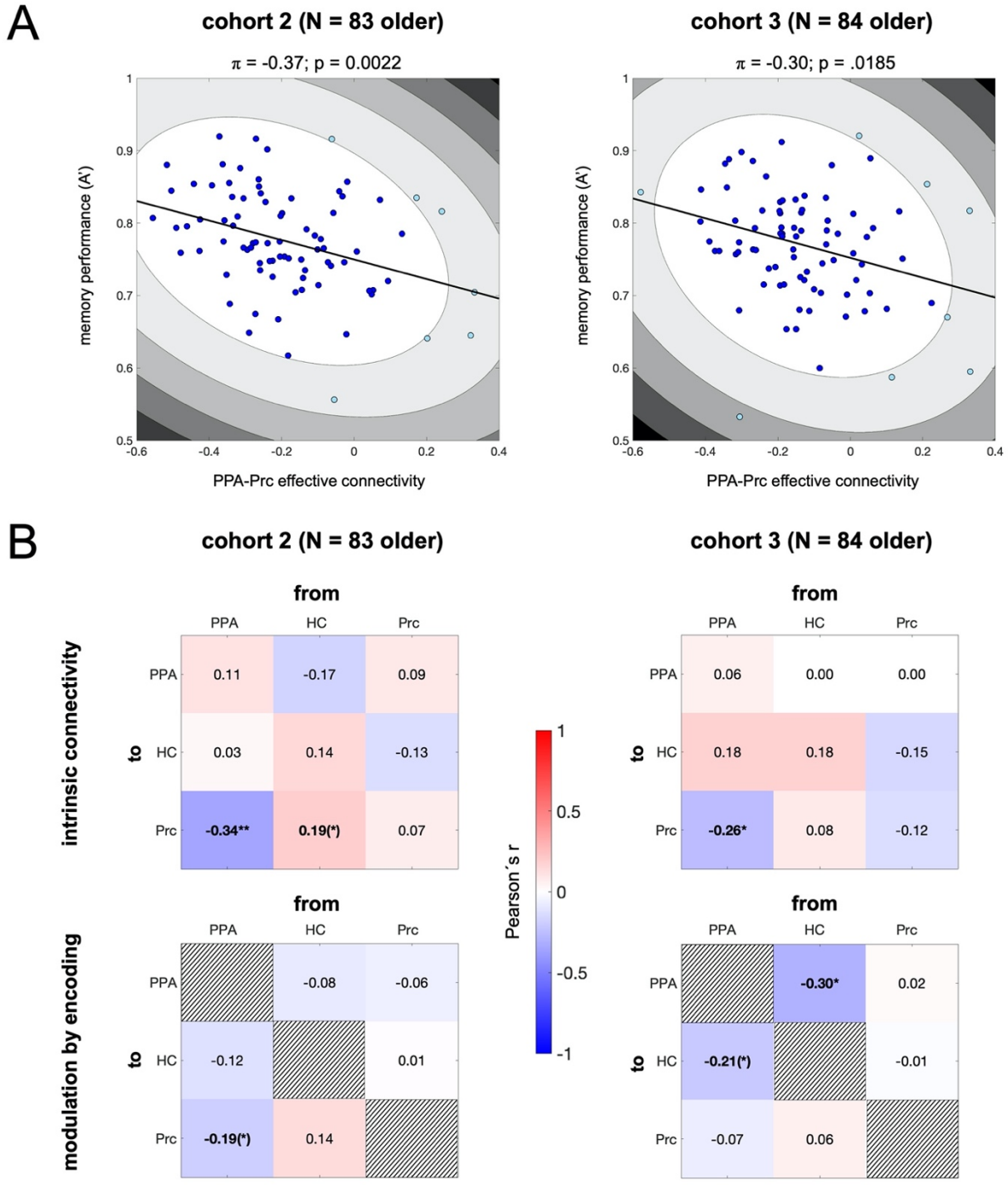

Figure 6. *Temporo-parietal effective connectivity during novelty processing and successful memory encoding.* Successful encoding was associated with increased activation of the hippocampus by the PPA and stronger suppression of the precuneus by the PPA. In older adults, the inhibitory connection from PPA to precuneus was attenuated and related to worse memory performance.

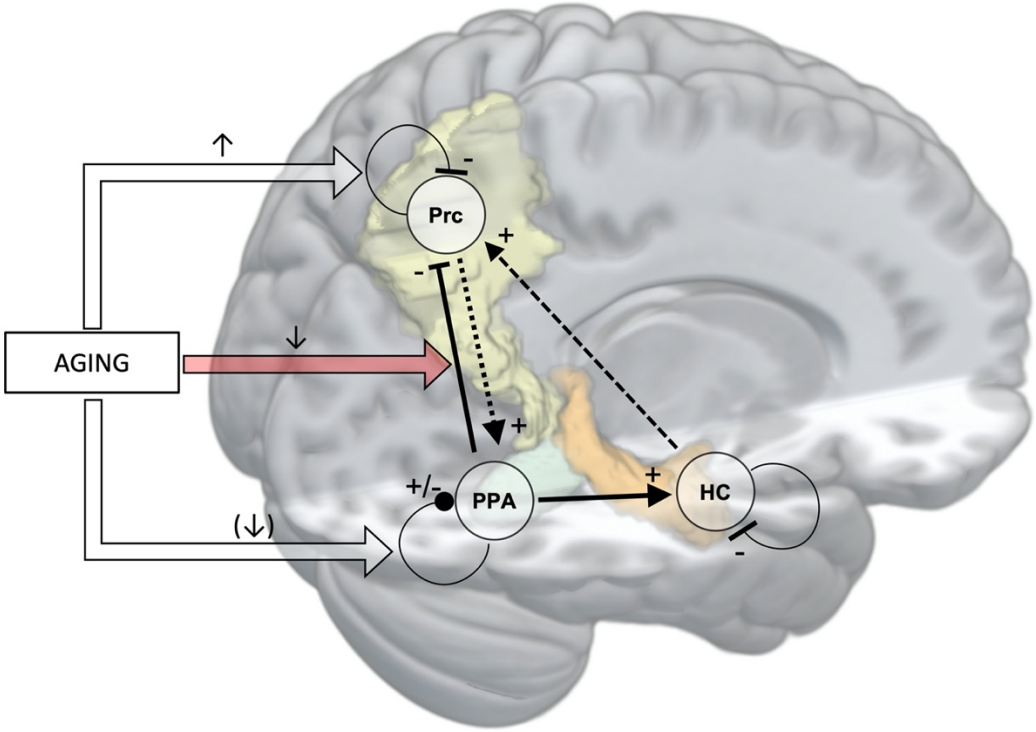

active during novelty processing, up-regulated during encoding

active during novelty processing, limited evidence for encoding-related up-regulation

active during novelty processing, no robust evidence for encoding-related modulation

self-connectivity (active during novelty processing, encoding-related modulation not tested)

7. Methods

7.1. Resource availability

7.1.1. Lead Contact

Further information and requests for resources should be directed to the lead contact, PD Dr. Dr. Björn H. Schott (bschott@lin-magdeburg.de).

7.1.2. Materials availability

This study did not generate plasmids, mouse lines, or unique reagents.

7.1.3. Data and code availability

Code: The code generated in the course of data analysis is available from the lead contact's GitHub site (URL to be provided upon acceptance).

Data: The single subjects' raw MRI data reported in this study cannot be deposited in a public repository due to EU data protection regulations. To request access, contact please contact the lead contact (bschott@lin-magdeburg.de). In addition, the DCM results reported in the present study have been deposited on NeuroVault (URL to be provided upon acceptance) and are publicly available as of the date of publication.

7.2. Experimental model and subject details

7.2.1. Participants

In the present study, we investigated three cohorts of participants, with the first cohort consisting of neurologically and psychiatrically healthy young adults (cohort 1: 117 young), and the other two cohorts including both young and older healthy participants (cohort 2: 58 young, 83 older; cohort 3: 64 young, 84 older). Participants were recruited via billboards, public outreach events of the Leibniz Institute for Neurobiology and local newspapers (for details on recruitment see (Richter et al., 2022; Soch et al., 2021a)). All participants were right-handed according to self-report. The Mini-International Neuropsychiatric Interview (M.I.N.I.; (Sheehan et al., 1998); German version by (Ackenheil et al., 1999) was used to exclude present or past psychiatric disorders. Further contraindications for participation included alcohol or drug abuse or the use of neurological or psychiatric medication. Data from sub-cohorts of the current study population have been reported in previous studies (cohort 1: (Assmann et al., 2021); cohort 2 and 3: (Richter et al., 2022; Soch et al., 2021a)). Importantly, the analyses performed here have not been conducted in the previous publications, and cohort 3 included 40

additional participants whose data have not been reported previously. Detailed demographic data are summarized in Table 1.

7.2.2. Informed consent and ethics approval

Written informed consent was obtained from all participants in accordance with the Declaration of Helsinki (2013), and the study was approved by the Ethics Committee of the Otto von Guericke University Magdeburg, Faculty of Medicine (Approval number 33/15).

7.3. Method details

7.3.1. Experimental paradigm

During the fMRI experiment, participants performed an incidental visual memory encoding paradigm, using an indoor/outdoor judgment as encoding task (Düzel et al., 2011). In cohort 1 (Assmann et al., 2021; Barman et al., 2014; Schott et al., 2014), the trial timings were slightly shorter compared to cohorts 2 and 3, where we employed the adapted version of the paradigm also used in the DELCODE study (Bainbridge et al., 2019; Düzel et al., 2022; Soch et al., 2021b) (see Table 1 for an overview of differences in trial timings and acquisition parameters). Subjects viewed photographs of indoor and outdoor scenes, which were either novel (44 indoor and outdoor scenes each) or were repetitions of two pre-familiarized "master" images (one indoor and one outdoor scene). Participants performed an "indoor" versus "outdoor" judgment on the images via button press. Each picture was presented for 2.5 s, followed by a variable delay ranging from 0.50 to 2.50 s in cohort 1 and from 0.70 s to 2.65 s in cohorts 2 and 3. The trial timing followed a near-exponential jitter and was optimized to improve estimation of the trial-specific BOLD responses (Hinrichs et al., 2000).

Approximately 70 min (cohorts 2, 3) to 90 min (cohort 1) after the start of the fMRI session, participants underwent a computer-based recognition memory test outside the scanner, during which they were presented with photographs from the fMRI encoding phase (*old*; n = 88 plus the two master images), randomly intermixed with previously unseen (*new*) images (n = 44). Participants reported their memory confidence orally on a five-point rating scale from 1 ("definitely new") to 5 ("definitely old"), and the overt responses were recorded by an experimenter. For details, also see Assmann et al. (Soch et al., 2021b) and Soch et al. (Soch et al., 2021a; Soch et al., 2021b).

7.3.2. MRI data acquisition

Structural and functional MRI data were acquired on two Siemens 3T MR tomographs (cohort 1 and 2: Siemens Verio; cohort 3: Siemens Skyra; see Table 1), using previously reported protocols (cohort 1: see (Assmann et al., 2021); cohorts 2 and 3: see (Soch et al., 2021b),

corresponding to the DELCODE MRI protocol, see (Düzel et al., 2018; Düzel et al., 2022; Jessen et al., 2018).

A T1-weighted MPRAGE image (TR = 2.5 s, TE = 4.37 ms, flip-α = 7°; 192 slices, 256 x 256 in-plane resolution, voxel size = 1 x 1 x 1 mm) was acquired for co-registration and improved spatial normalization. In cohorts 2 and 3, phase and magnitude fieldmap images were acquired to improve correction for artifacts resulting from magnetic field inhomogeneities (*unwarping*, see below).

For functional MRI (fMRI), 206 T2*-weighted echo-planar images were acquired in interleaved-ascending slice order (see Table 1 for acquisition details). The complete study protocol also included additional structural MR images, which were not used in the analyses reported here (details available upon request).

7.3.3. fMRI data preprocessing

Data preprocessing and analysis was performed using Statistical Parametric Mapping (SPM12; University College London; https://www.fil.ion.ucl.ac.uk/spm/software/spm12/) running on MATLAB R2018b (Mathworks, Natick, MA). EPIs were corrected for acquisition time delay (*slice timing*), head motion (*realignment*) and magnetic field inhomogeneities (*unwarping*), using voxel-displacement maps (VDMs) derived from the fieldmaps (cohorts 2 and 3). The MPRAGE image was spatially co-registered to the mean realigned (cohort 1) or *unwarped* (cohorts 2 and 3) image and *segmented* into six tissue types, using the unified segmentation and normalization algorithm implemented in SPM12. The resulting forward deformation parameters were used to *normalize* EPIs into a standard stereotactic reference frame (Montreal Neurological Institute, MNI; voxel size = 3 x 3 x 3 mm). Normalized images were spatially *smoothed* using an isotropic Gaussian kernel of 6 mm full width at half maximum (FWHM).

7.4. Quantification and statistical analysis

7.4.1. General linear model (GLM)-based fMRI data analysis

Statistical analysis of fMRI data was performed based on a two-stage mixed-effects model as implemented in SPM12. At the first stage (single-subject level), we used a parametric general linear model (GLM) of the subsequent memory effect that has previously been demonstrated to outperform the commonly employed categorical models (Soch et al., 2021b). The model included two onset regressors, one for novel images ("novelty regressor") and one for presentations of the two pre-familiarized images ("master regressor"). Both regressors consisted of short box-car stimulus functions (2.5 s), which were convolved with the canonical hemodynamic response function (HRF), as implemented in SPM12.

The regressor reflecting subsequent memory performance was obtained by parametrically modulating the novelty regressor with an arcsine function describing subsequent recognition confidence. Specifically, the parametric modulator (PM) was given by

$$\mathrm{PM} = \arcsin\left(\frac{x-3}{2}\right) \cdot \frac{2}{\pi}$$

where $x \in \{1, 2, 3, 4, 5\}$ is the subsequent memory report, such that $-1 \leq \mathrm{PM} \leq +1$. By employing the arcsine transformation, *definitely* remembered (response "5") or forgotten (response "1") items were weighted more strongly than *probably* remembered (response "4") or forgotten (response "2") items ((Soch et al., 2021b), Fig. 2A). The model also included the six rigid-body movement parameters obtained from realignment as covariates of no interest and a constant representing the implicit baseline.

At the second stage of the model (across-subject level), contrasts of interest (novelty contrast: novel vs. master images; memory contrast: parametric memory regressor) were submitted to a one-sample t-test (cohort 1) and to ANCOVA models with age group as between-subjects factor and gender as a binary covariate of no interest (cohort 2, 3), respectively. The significance level was set to $p < .05$, whole-brain-corrected for family-wise error (FWE) at voxel-level, with a minimum cluster size of $k = 10$ adjacent voxels.

7.4.2. Dynamic Causal Modeling

Effective connectivity analysis was performed using DCM version 12.5 as implemented in SPM12. DCM uses an input-state-output model based on a bilinear state equation:

$$\dot{z} = \left(A + \sum_{j=1}^{M} \mathrm{u}_j \mathrm{B}^{(j)}\right) z + Cu$$

where $\dot{z}$ is the temporal derivative of the state variable z, which describes neuronal activity resulting from intrinsic effective connectivity (A), changes in connectivity due to the contextual modulations (B) and the direct influence of the driving input u (C). The thus defined neuronal model is coupled to a biologically plausible neurovascular model of the BOLD response, and the coupled models are used to predict the BOLD time series in *a priori* defined volumes of interest (VOIs).

The goal of our DCM analysis was two-fold:

1. First, we aimed to assess the intrinsic effective connectivity of the PPA, the HC, and the Prc during novelty processing and the connectivity changes related to successful versus unsuccessful encoding of novel visual information.

2. Second, we aimed to assess, which connections within a temporo-parietal memory network are affected by age and whether age-related differences in effective connectivity are associated with memory performance in older adults.

Definition of regions of interest and time series extraction

ROIs were defined based on both anatomical and functional criteria: Anatomical constraints were defined using anatomical ROIs taken from Automated Anatomical Labeling (AAL), a canonical parcellation of the human brain (Tzourio-Mazoyer et al., 2002), as implemented in the WFU PickAtlas (Wake Forest University; https://www.nitrc.org/ projects/wfu_pickatlas/) or from previously described literature-based ROIs. Functional constraints were derived of memory and novelty contrasts in a previously published subset of cohorts 2 and 3 (106 young and 111 older participants; (Soch et al., 2021a; Soch et al., 2021b)). Based on the meta-analytic evidence on encoding-related activations and deactivations (Kim, 2011) and the age-related changes of those patterns (Maillet and Rajah, 2014), and guided by our own replication of those results, the ROIs were generated as follows:

1. The PPA, which showed a pronounced response during both novelty detection and successful encoding (Soch et al., 2021a) was used as the network's driving input region, given its well-replicated and relatively specific response to scene stimuli (Epstein and Baker, 2019) and particularly to novel scenes (Bunzeck et al., 2006; Epstein, 2008). Given that the definition of the PPA is mainly based on its responsivity to scene stimuli rather than on anatomical landmarks, we restricted our ROI to a probabilistic definition of the PPA based on local maxima of activation clusters that were shown to respond to scene stimuli in previous studies (for details see (Zweynert et al., 2011)). This probabilistic ROI was further restricted to the anatomical boundaries of the fusiform and parahippocampal gyri as defined by the AAL parcellation. Considering the intended use of the PPA as input region responding to all presentations of novel scenes (i.e. irrespective of subsequent encoding success), the thresholded SPM for the novelty contrast (novel > master images) was multiplied with the mask of the PPA, yielding a ROI for the PPA.
2. The HC has repeatedly been shown to respond more strongly to subsequently remembered compared to subsequently forgotten information in both young and older adults (Kim, 2011; Maillet and Rajah, 2014), a finding replicated in the present study (Figure 2). The ROI for the HC was thus defined by multiplying the thresholded SPM for the memory contrast (positive effects of the parametric memory regressor) with the anatomical boundaries of the

HC from the AAL atlas and with a sphere seeded at the local group maximum of the contrast within the right anterior HC ([x y z] = [21 -10 -19]; r = 15 mm).

3. The Prc emerged as the region most robustly activating more strongly (or, deactivating less strongly) during successful memory formation in older rather than young adults (Figure 2), in line with previous meta-analytic observations (Maillet and Rajah, 2014). We thus inclusively masked the thresholded SPM for the age group contrast (older > young) from the second-level memory GLM with the AAL Prc mask. To exclude activations in more lateral parietal cortex and posterior cingulate cortex, we further restricted the Prc ROI to a sphere centered at the local maximum of the age contrast ([x y z] = [6 -64 38]; r = 18 mm).

To improve signal-to-noise ratio (SNR), we further restricted the ROIs to voxels with an uncorrected $p < 0.25$ on the respective contrast in the first-level GLM of each subject. The first eigenvariate time series were extracted from the thus obtained volumes of interest (VOIs) and adjusted for effects of interest (EOI) modeled and explained by the individual first-level GLMs.

First-level DCM analysis

The Parametric Empirical Bayes (PEB) framework implemented in SPM12 (Zeidman et al., 2019a; Zeidman et al., 2019b) allows for an efficient estimation of effective connectivity at group level by estimating the full model for each individual subject and pruning parameters that do not contribute to the model quality at the second level. In the present study, we employed bilinear DCM as implemented in the DCM PEB framework ((Zeidman et al., 2019a); cf. eq. 2}), similarly to previous descriptions of the approach (Bencivenga et al., 2021; Sacu et al., 2022).

The most general model which was estimated for each subject included the ROIs of the HC, PPA, and Prc, assuming full intrinsic connectivity, including self-connections. Novelty (i.e. presentation of novel, but not *master* images) was chosen as driving input to the PPA, and memory (the arcsine-transformed recognition memory responses representing encoding success) was included as a potential contextual modulator at all between-regions connections, but not at the self-connections (Figure 1, right). Neural responses to the highly familiar *master* images were not included in the model and thus formed the implicit baseline (Zeidman et al., 2019a). The slice timing model implemented in the DCM PEB framework (Kiebel et al., 2007) was set to the last acquired slice (Seghier et al., 2011; Zeidman et al., 2019a). This was motivated by the fact that the stimulus duration (2.5 s) was close to the TR, and mini-blocks of 2.5 s provided a better model fit than delta functions in first-level GLM analysis (Soch et al.,

2021b).[2] Model estimation was performed using variational Laplace (Friston et al., 2016), which provides both, posterior estimates of connection strengths and the free energy approximation to the marginal likelihood (Friston et al., 2007). To yield a higher proportion of explained variance at the single-subject level, an iterative fit was performed, using the group mean parameter estimates as empirical priors (SPM function *spm_dcm_peb_fit.m*; (Zeidman et al., 2019b)).

Group-level inference

Group-level inference on the effective connectivity within the temporo-parietal network was performed using Bayesian model reduction (BMR) and averaging (BMA), as implemented in the DCM PEB framework (Friston et al., 2016; Zeidman et al., 2019b). After estimating each participant's full model (allowing for all potential connections and contextual modulations), the thus obtained DCMs were submitted to a second-level Bayesian GLM (Dijkstra et al., 2017; Zeidman et al., 2019b). To assess the strength of effective connectivity between the three ROIs as well as their modulation by successful memory performance and aging, the 15 parameters from model inversion (A-matrix and B-matrix) were submitted to BMR, followed by BMA. BMR compares the full model with a model space of nested models where one or more parameters (i.e. connections or contextual modulations) are switched off, keeping the parameters with the most evidence (Friston and Penny, 2011; Friston et al., 2016; Zeidman et al., 2019b). Subsequently, BMA was employed to average the parameters across models, weighted by the evidence of each model (Penny et al., 2010; Zeidman et al., 2019b). To test parameters across (or between) groups, we thresholded the posterior probability (PP) at 0.95 for any given parameter (or parameter difference) being larger than zero ($PP = \Pr(\theta > 0|y) > 0.95$). While it is commonly recommended to use a threshold based on free energy, this approximation is vulnerable to local minima during group model comparison (Wei et al., 2020; Zeidman et al., 2019a) and may thus reduce the generalizability. Parameters with supra-threshold PP in all three cohorts (or in cohorts 2 and 3, when testing for age group effects) were considered robust, and parameters with a PP > 0.95 in two cohorts were considered limited evidence.

[2] As a control, we also computed DCMs using $TR/2$ and TR/N_{slices} (i.e., number of slices) in the slice timing model. Explained variance of the first-level DCM analyses was substantially poorer for TR/N_{slices} (cohort 1: p = .001; cohort 2: p = .057; cohort 3: p < .001) and did not differ significantly for $TR/2$ (all > .161). Results of second-level PEB analysis for the model using $TR/2$ were qualitatively highly similar to the results of that using TR reported here.

We additionally computed one-sample t-tests for all parameters against baseline and two-sample t-tests for age group differences to evaluate the agreement between Bayesian and classical inferential statistics.

7.4.3. Prediction of memory performance from DCM parameters

After group-level PEB analysis, we assessed whether the estimated parameters were associated with memory performance in older adults, and thereby contribute to assess the neurobiological underpinnings of cognitive aging.

Memory performance estimate

To obtain a measure of memory performance that takes into account recognition confidence, the area under the curve plotting hits (i.e., correctly recognized previously seen stimuli) against false alarms (i.e., falsely recognized previously unseen stimuli) was calculated as described previously ((Soch et al., 2021a), Appendix B). To this end, $o_1, \dots, o_5$ and $n_1, \dots, n_5$ were defined as the numbers of old stimuli and new stimuli, respectively, rated as 1 ("definitely new") to 5 ("definitely old") in the delayed recognition test. Hit rates (H) and false alarm (FA) rates as functions of a threshold $t \in \{0,1, \dots ,5\}$ are defined as proportions of old and new stimuli, respectively, rated higher than t:

$$\mathrm{H}(t) = \frac{1}{O}\sum_{i=t+1}^{5} o_i$$

$$\mathrm{FA}(t) = \frac{1}{N}\sum_{i=t+1}^{5} n_i$$

where $O = o_1 + \cdots + o_5$ and $N = n_1 + \cdots + n_5$. Note that $\mathrm{H}(0) = \mathrm{FA}(0) = 1$ and $\mathrm{H}(5) = \mathrm{FA}(5) = 0$. The hit rate can then be expressed as a function of the FA rate:

$$y = f(x), \text{ such that } y = \mathrm{H}(t) \text{ and } x = \mathrm{FA}(t) \text{ for each } t = 0,1, \dots ,5$$

The area under the ROC curve (AUC) is then obtained by computing the integral of this function from 0 to 1:

$$A' = \int_0^1 f(x)\,\mathrm{d}x = \int_0^1 \mathrm{H}(\mathrm{FA})\,\mathrm{dFA}$$

The value of this integral is referred to as AUC or ffA' ("A-prime") and provides a measure for memory performance, similar to the corrected hit rate, but also accounting for recognition confidence. When responses are completely random, A' equals 0.5, reflecting pure guessing. When all old items are recognized and all new items are correctly rejected, A' equals 1, reflecting 100% performance. An advantage over the frequently employed d' measure (MacMillan, 1991) is that A' has finite values even in cases of zero or perfect performance.

Brain-behavior correlations

We computed outlier-robust Shepherd's *Pi* correlations (Schwarzkopf et al., 2012) between connections that showed a robust age-group-related difference – as defined in 2.6.3 – and A' as a memory measure. Shepherd's *Pi* correlations have been proposed as a method to improve reliability of brain-behavior correlations, which have been criticized for their lack of robustness (Yarkoni, 2009) and susceptibility to outliers (Rousselet and Pernet, 2012; Schwarzkopf et al., 2012). The approach is based on Spearman's correlation and includes a bootstrap-based estimation of the Mahalanobis distance, thereby allowing for an unbiased detection and exclusion of outliers.

To further explore which DCM parameters were associated with memory performance in older adults, we computed Pearson's correlations between all DCM parameters and A' as the memory measure of interest, using the false discovery rate (FDR) correction for multiple comparisons (Benjamini and Hochberg, 1995).

8. References

(2013). World Medical Association Declaration of Helsinki: ethical principles for medical research involving human subjects. Jama *310*, 2191-2194.

Ackenheil, M., Stotz, G., Dietz-Bauer, R., Vossen, A., Dietz, R., Vossen-Wellmann, A., and Vossen, J.A. (1999). Mini International Neuropsychiatric Interview. German Version 5.0.0, DSM-IV (München: Psychiatrische Universitätsklinik München).

Aminoff, E.M., Kveraga, K., and Bar, M. (2013). The role of the parahippocampal cortex in cognition. Trends Cogn Sci *17*, 379-390.

Assmann, A., Richter, A., Schütze, H., Soch, J., Barman, A., Behnisch, G., Knopf, L., Raschick, M., Schult, A., Wüstenberg, T.*, et al.* (2021). Neurocan genome-wide psychiatric risk variant affects explicit memory performance and hippocampal function in healthy humans. Eur J Neurosci *53*, 3942-3959.

Bainbridge, W.A., Berron, D., Schütze, H., Cardenas-Blanco, A., Metzger, C., Dobisch, L., Bittner, D., Glanz, W., Spottke, A., Rudolph, J.*, et al.* (2019). Memorability of photographs in subjective cognitive decline and mild cognitive impairment: Implications for cognitive assessment. Alzheimers Dement (Amst) *11*, 610-618.

Barman, A., Assmann, A., Richter, S., Soch, J., Schütze, H., Wüstenberg, T., Deibele, A., Klein, M., Richter, A., Behnisch, G.*, et al.* (2014). Genetic variation of the RASGRF1 regulatory region affects human hippocampus-dependent memory. Front Hum Neurosci *8*, 260.

Beason-Held, L.L., Shafer, A.T., Goh, J.O., Landman, B.A., Davatzikos, C., Viscomi, B., Ash, J., Kitner-Triolo, M., Ferrucci, L., and Resnick, S.M. (2021). Hippocampal activation and connectivity in the aging brain. Brain Imaging Behav *15*, 711-726.

Bencivenga, F., Sulpizio, V., Tullo, M.G., and Galati, G. (2021). Assessing the effective connectivity of premotor areas during real vs imagined grasping: a DCM-PEB approach. Neuroimage *230*, 117806.

Benjamini, Y., and Hochberg, Y. (1995). Controlling the False Discovery Rate: A Practical and Powerful Approach to Multiple Testing. Journal of the Royal Statistical Society Series B (Methodological) *57*, 289-300.

Billette, O.V., Ziegler, G., Aruci, M., Schütze, H., Kizilirmak, J.M., Richter, A., Altenstein, S., Bartels, C., Brosseron, F., Cardenas-Blanco, A.*, et al.* (2022). Novelty-Related fMRI Responses of Precuneus and Medial Temporal Regions in Individuals at Risk for Alzheimer Disease. Neurology *99*, e775-e788.

Brewer, J.B., Zhao, Z., Desmond, J.E., Glover, G.H., and Gabrieli, J.D. (1998). Making memories: brain activity that predicts how well visual experience will be remembered. Science *281*, 1185-1187.

Brodt, S., Gais, S., Beck, J., Erb, M., Scheffler, K., and Schönauer, M. (2018). Fast track to the neocortex: A memory engram in the posterior parietal cortex. Science *362*, 1045-1048.

Brodt, S., Pöhlchen, D., Flanagin, V.L., Glasauer, S., Gais, S., and Schönauer, M. (2016). Rapid and independent memory formation in the parietal cortex. Proc Natl Acad Sci U S A *113*, 13251-13256.

Buckner, R.L., Andrews-Hanna, J.R., and Schacter, D.L. (2008). The brain's default network: anatomy, function, and relevance to disease. Ann N Y Acad Sci *1124*, 1-38.

Bunzeck, N., Schütze, H., and Düzel, E. (2006). Category-specific organization of prefrontal response-facilitation during priming. Neuropsychologia *44*, 1765-1776.

Cabeza, R., Albert, M., Belleville, S., Craik, F.I.M., Duarte, A., Grady, C.L., Lindenberger, U., Nyberg, L., Park, D.C., Reuter-Lorenz, P.A.*, et al.* (2018). Maintenance, reserve and compensation: the cognitive neuroscience of healthy ageing. Nat Rev Neurosci *19*, 701-710.

Chen, X., Varghese, L., and Jagust, W.J. (2022). A Double-Edged Sword: The Role of Prior Knowledge in Memory Aging. Front Aging Neurosci *14*, 874767.

Cohen, M.X. (2011). Hippocampal-prefrontal connectivity predicts midfrontal oscillations and long-term memory performance. Curr Biol *21*, 1900-1905.

Cooper, R.A., and Ritchey, M. (2019). Cortico-hippocampal network connections support the multidimensional quality of episodic memory. Elife *8*.

Daunizeau, J., David, O., and Stephan, K.E. (2011). Dynamic causal modelling: a critical review of the biophysical and statistical foundations. Neuroimage *58*, 312-322.

Dennis, N.A., Hayes, S.M., Prince, S.E., Madden, D.J., Huettel, S.A., and Cabeza, R. (2008). Effects of aging on the neural correlates of successful item and source memory encoding. J Exp Psychol Learn Mem Cogn *34*, 791-808.

Deshpande, G., Zhao, X., and Robinson, J. (2022). Functional parcellation of the hippocampus based on its layer-specific connectivity with default mode and dorsal attention networks. Neuroimage *254*, 119078.

Diersch, N., Valdes-Herrera, J.P., Tempelmann, C., and Wolbers, T. (2021). Increased Hippocampal Excitability and Altered Learning Dynamics Mediate Cognitive Mapping Deficits in Human Aging. J Neurosci *41*, 3204-3221.

Dijkstra, N., Zeidman, P., Ondobaka, S., van Gerven, M.A.J., and Friston, K. (2017). Distinct Top-down and Bottom-up Brain Connectivity During Visual Perception and Imagery. Sci Rep *7*, 5677.

Düzel, E., Berron, D., Schütze, H., Cardenas-Blanco, A., Metzger, C., Betts, M., Ziegler, G., Chen, Y., Dobisch, L., Bittner, D.*, et al.* (2018). CSF total tau levels are associated with hippocampal novelty irrespective of hippocampal volume. Alzheimers Dement (Amst) *10*, 782-790.

Düzel, E., Schütze, H., Yonelinas, A.P., and Heinze, H.J. (2011). Functional phenotyping of successful aging in long-term memory: Preserved performance in the absence of neural compensation. Hippocampus *21*, 803-814.

Düzel, E., Ziegler, G., Berron, D., Maass, A., Schütze, H., Cardenas-Blanco, A., Glanz, W., Metzger, C., Dobisch, L., Reuter, M.*, et al.* (2022). Amyloid pathology but not APOE ε4 status is permissive for tau-related hippocampal dysfunction. Brain *145*, 1473-1485.

Eichenbaum, H., Yonelinas, A.P., and Ranganath, C. (2007). The medial temporal lobe and recognition memory. Annu Rev Neurosci *30*, 123-152.

Epstein, R.A. (2008). Parahippocampal and retrosplenial contributions to human spatial navigation. Trends Cogn Sci *12*, 388-396.

Epstein, R.A., and Baker, C.I. (2019). Scene Perception in the Human Brain. Annu Rev Vis Sci *5*, 373-397.

Friston, K., Mattout, J., Trujillo-Barreto, N., Ashburner, J., and Penny, W. (2007). Variational free energy and the Laplace approximation. Neuroimage *34*, 220-234.

Friston, K., and Penny, W. (2011). Post hoc Bayesian model selection. Neuroimage *56*, 2089-2099.

Friston, K.J., Litvak, V., Oswal, A., Razi, A., Stephan, K.E., van Wijk, B.C.M., Ziegler, G., and Zeidman, P. (2016). Bayesian model reduction and empirical Bayes for group (DCM) studies. Neuroimage *128*, 413-431.

Fuentemilla, L., Càmara, E., Münte, T.F., Krämer, U.M., Cunillera, T., Marco-Pallarés, J., Tempelmann, C., and Rodriguez-Fornells, A. (2009). Individual differences in true and false memory retrieval are related to white matter brain microstructure. J Neurosci *29*, 8698-8703.

Gilmore, A.W., Nelson, S.M., and McDermott, K.B. (2015). A parietal memory network revealed by multiple MRI methods. Trends Cogn Sci *19*, 534-543.

Grady, C.L., Springer, M.V., Hongwanishkul, D., McIntosh, A.R., and Winocur, G. (2006). Age-related changes in brain activity across the adult lifespan. J Cogn Neurosci *18*, 227-241.

Hafkemeijer, A., van der Grond, J., and Rombouts, S.A. (2012). Imaging the default mode network in aging and dementia. Biochim Biophys Acta *1822*, 431-441.

Henke, K. (2010). A model for memory systems based on processing modes rather than consciousness. Nat Rev Neurosci *11*, 523-532.

Hinrichs, H., Scholz, M., Tempelmann, C., Woldorff, M.G., Dale, A.M., and Heinze, H.J. (2000). Deconvolution of event-related fMRI responses in fast-rate experimental designs: tracking amplitude variations. J Cogn Neurosci *12 Suppl 2*, 76-89.

Jessen, F., Spottke, A., Boecker, H., Brosseron, F., Buerger, K., Catak, C., Fliessbach, K., Franke, C., Fuentes, M., Heneka, M.T.*, et al.* (2018). Design and first baseline data of the DZNE multicenter observational study on predementia Alzheimer's disease (DELCODE). Alzheimers Res Ther *10*, 15.

Kernbach, J.M., Yeo, B.T.T., Smallwood, J., Margulies, D.S., Thiebaut de Schotten, M., Walter, H., Sabuncu, M.R., Holmes, A.J., Gramfort, A., Varoquaux, G.*, et al.* (2018). Subspecialization within default mode nodes characterized in 10,000 UK Biobank participants. Proc Natl Acad Sci U S A *115*, 12295-12300.

Kiebel, S.J., Klöppel, S., Weiskopf, N., and Friston, K.J. (2007). Dynamic causal modeling: a generative model of slice timing in fMRI. Neuroimage *34*, 1487-1496.

Kim, H. (2011). Neural activity that predicts subsequent memory and forgetting: a meta-analysis of 74 fMRI studies. Neuroimage *54*, 2446-2461.

Kinnavane, L., Amin, E., Horne, M., and Aggleton, J.P. (2014). Mapping parahippocampal systems for recognition and recency memory in the absence of the rat hippocampus. Eur J Neurosci *40*, 3720-3734.

Kizilirmak, J., Soch, J., Schütze, H., Düzel, E., Feldhoff, H., Fischer, L., Knopf, L., Maass, A., Raschick, M., Schult, A.*, et al.* (2022). The relationship between resting-state amplitude fluctuations and memory-related deactivations of the Default Mode Network in young and older adults. PsyArXiv.

Kizilirmak, J.M., Fischer, L., Krause, J., Soch, J., Richter, A., and Schott, B.H. (2021). Learning by Insight-Like Sudden Comprehension as a Potential Strategy to Improve Memory Encoding in Older Adults. Front Aging Neurosci *13*, 661346.

Knights, E., Morcom, A.M., and Henson, R.N. (2021). Does Hemispheric Asymmetry Reduction in Older Adults in Motor Cortex Reflect Compensation? J Neurosci *41*, 9361-9373.

Köhler, S., Crane, J., and Milner, B. (2002). Differential contributions of the parahippocampal place area and the anterior hippocampus to human memory for scenes. Hippocampus *12*, 718-723.

Kremers, N.A., Deuker, L., Kranz, T.A., Oehrn, C., Fell, J., and Axmacher, N. (2014). Hippocampal control of repetition effects for associative stimuli. Hippocampus *24*, 892-902.

Kumaran, D., and Maguire, E.A. (2007). Match mismatch processes underlie human hippocampal responses to associative novelty. J Neurosci *27*, 8517-8524.

Li, Y., Cheng, J.X., and Yu, J. (2022). Episodic memory updating among older adults: moderating role of prior knowledge. Memory, 1-8.

Lohmann, G., Erfurth, K., Müller, K., and Turner, R. (2012). Critical comments on dynamic causal modelling. Neuroimage *59*, 2322-2329.

Lyu, D., Pappas, I., Menon, D.K., and Stamatakis, E.A. (2021). A Precuneal Causal Loop Mediates External and Internal Information Integration in the Human Brain. J Neurosci *41*, 9944-9956.

MacMillan, N.A.C., C. D. (1991). Detection theory: A user's guide (New York: Cambridge University Press).

Maillet, D., and Rajah, M.N. (2014). Age-related differences in brain activity in the subsequent memory paradigm: a meta-analysis. Neurosci Biobehav Rev *45*, 246-257.

Malagurski, B., Liem, F., Oschwald, J., Mérillat, S., and Jäncke, L. (2020). Functional dedifferentiation of associative resting state networks in older adults - A longitudinal study. Neuroimage *214*, 116680.

Marks, W.D., Yamamoto, N., and Kitamura, T. (2021). Complementary roles of differential medial entorhinal cortex inputs to the hippocampus for the formation and integration of temporal and contextual memory (Systems Neuroscience). Eur J Neurosci *54*, 6762-6779.

Morcom, A.M., Good, C.D., Frackowiak, R.S., and Rugg, M.D. (2003). Age effects on the neural correlates of successful memory encoding. Brain *126*, 213-229.

Nyberg, L. (2017). Functional brain imaging of episodic memory decline in ageing. J Intern Med *281*, 65-74.

Nyberg, L., Andersson, M., Lundquist, A., Salami, A., and Wåhlin, A. (2019). Frontal Contribution to Hippocampal Hyperactivity During Memory Encoding in Aging. Front Mol Neurosci *12*, 229.

Olarte-Sánchez, C.M., Kinnavane, L., Amin, E., and Aggleton, J.P. (2014). Contrasting networks for recognition memory and recency memory revealed by immediate-early gene imaging in the rat. Behav Neurosci *128*, 504-522.

Paller, K.A., Kutas, M., and Mayes, A.R. (1987). Neural correlates of encoding in an incidental learning paradigm. Electroencephalogr Clin Neurophysiol *67*, 360-371.

Penny, W.D., Stephan, K.E., Daunizeau, J., Rosa, M.J., Friston, K.J., Schofield, T.M., and Leff, A.P. (2010). Comparing families of dynamic causal models. PLoS Comput Biol *6*, e1000709.

Penny, W.D., Stephan, K.E., Mechelli, A., and Friston, K.J. (2004). Modelling functional integration: a comparison of structural equation and dynamic causal models. Neuroimage *23 Suppl 1*, S264-274.

Qin, P., Liu, Y., Shi, J., Wang, Y., Duncan, N., Gong, Q., Weng, X., and Northoff, G. (2012). Dissociation between anterior and posterior cortical regions during self-specificity and familiarity: a combined fMRI-meta-analytic study. Hum Brain Mapp *33*, 154-164.

Ranganath, C., and Rainer, G. (2003). Neural mechanisms for detecting and remembering novel events. Nat Rev Neurosci *4*, 193-202.

Ranganath, C., and Ritchey, M. (2012). Two cortical systems for memory-guided behaviour. Nat Rev Neurosci *13*, 713-726.

Renoult, L., Irish, M., Moscovitch, M., and Rugg, M.D. (2019). From Knowing to Remembering: The Semantic-Episodic Distinction. Trends Cogn Sci *23*, 1041-1057.

Richter, A., Soch, J., Kizilirmak, J.M., Fischer, L., Schütze, H., Assmann, A., Behnisch, G., Feldhoff, H., Knopf, L., Raschick, M.*, et al.* (2022). Single-value scores of memory-related brain activity reflect dissociable neuropsychological and anatomical signatures of neurocognitive aging. bioRxiv, 2022.2002.2004.479169.

Rousselet, G.A., and Pernet, C.R. (2012). Improving standards in brain-behavior correlation analyses. Front Hum Neurosci *6*, 119.

Sacu, S., Wackerhagen, C., Erk, S., Romanczuk-Seiferth, N., Schwarz, K., Schweiger, J.I., Tost, H., Meyer-Lindenberg, A., Heinz, A., Razi, A.*, et al.* (2022). Effective connectivity during face processing in major depression - distinguishing markers of pathology, risk, and resilience. Psychol Med, 1-13.

Sambataro, F., Murty, V.P., Callicott, J.H., Tan, H.Y., Das, S., Weinberger, D.R., and Mattay, V.S. (2010). Age-related alterations in default mode network: impact on working memory performance. Neurobiol Aging *31*, 839-852.

Schott, B.H., Assmann, A., Schmierer, P., Soch, J., Erk, S., Garbusow, M., Mohnke, S., Pöhland, L., Romanczuk-Seiferth, N., Barman, A.*, et al.* (2014). Epistatic interaction of genetic depression risk variants in the human subgenual cingulate cortex during memory encoding. Transl Psychiatry *4*, e372.

Schott, B.H., Niklas, C., Kaufmann, J., Bodammer, N.C., Machts, J., Schütze, H., and Düzel, E. (2011). Fiber density between rhinal cortex and activated ventrolateral prefrontal regions predicts episodic memory performance in humans. Proc Natl Acad Sci U S A *108*, 5408-5413.

Schott, B.H., Wüstenberg, T., Lücke, E., Pohl, I.M., Richter, A., Seidenbecher, C.I., Pollmann, S., Kizilirmak, J.M., and Richardson-Klavehn, A. (2019). Gradual acquisition of visuospatial associative memory representations via the dorsal precuneus. Hum Brain Mapp *40*, 1554-1570.

Schott, B.H., Wüstenberg, T., Wimber, M., Fenker, D.B., Zierhut, K.C., Seidenbecher, C.I., Heinze, H.J., Walter, H., Düzel, E., and Richardson-Klavehn, A. (2013). The relationship between level of processing and hippocampal-cortical functional connectivity during episodic memory formation in humans. Hum Brain Mapp *34*, 407-424.

Schwarzkopf, D.S., De Haas, B., and Rees, G. (2012). Better ways to improve standards in brain-behavior correlation analysis. Front Hum Neurosci *6*, 200.

Seghier, M.L., Josse, G., Leff, A.P., and Price, C.J. (2011). Lateralization is predicted by reduced coupling from the left to right prefrontal cortex during semantic decisions on written words. Cereb Cortex *21*, 1519-1531.

Sheehan, D.V., Lecrubier, Y., Sheehan, K.H., Amorim, P., Janavs, J., Weiller, E., Hergueta, T., Baker, R., and Dunbar, G.C. (1998). The Mini-International Neuropsychiatric Interview (M.I.N.I.): the development and validation of a structured diagnostic psychiatric interview for DSM-IV and ICD-10. J Clin Psychiatry *59 Suppl 20*, 22-33;quiz 34-57.

Snyder, A.D., Ma, L., Steinberg, J.L., Woisard, K., and Moeller, F.G. (2021). Dynamic Causal Modeling Self-Connectivity Findings in the Functional Magnetic Resonance Imaging Neuropsychiatric Literature. Front Neurosci *15*, 636273.

Soch, J., Richter, A., Kizilirmak, J.M., Schütze, H., Feldhoff, H., Fischer, L., Knopf, L., Raschick, M., Schult, A., Düzel, E.*, et al.* (2022). Structural and functional MRI data differentially predict chronological age and behavioral memory performance. eNeuro.

Soch, J., Richter, A., Schütze, H., Kizilirmak, J.M., Assmann, A., Behnisch, G., Feldhoff, H., Fischer, L., Heil, J., Knopf, L.*, et al.* (2021a). A comprehensive score reflecting memory-related fMRI activations and deactivations as potential biomarker for neurocognitive aging. Hum Brain Mapp *42*, 4478-4496.

Soch, J., Richter, A., Schütze, H., Kizilirmak, J.M., Assmann, A., Knopf, L., Raschick, M., Schult, A., Maass, A., Ziegler, G.*, et al.* (2021b). Bayesian model selection favors parametric over categorical fMRI subsequent memory models in young and older adults. Neuroimage *230*, 117820.

Sperling, R.A., Laviolette, P.S., O'Keefe, K., O'Brien, J., Rentz, D.M., Pihlajamaki, M., Marshall, G., Hyman, B.T., Selkoe, D.J., Hedden, T.*, et al.* (2009). Amyloid deposition is associated with impaired default network function in older persons without dementia. Neuron *63*, 178-188.

Stark, S.M., Frithsen, A., and Stark, C.E.L. (2021). Age-related alterations in functional connectivity along the longitudinal axis of the hippocampus and its subfields. Hippocampus *31*, 11-27.

Tzourio-Mazoyer, N., Landeau, B., Papathanassiou, D., Crivello, F., Etard, O., Delcroix, N., Mazoyer, B., and Joliot, M. (2002). Automated anatomical labeling of activations in SPM using a macroscopic anatomical parcellation of the MNI MRI single-subject brain. Neuroimage *15*, 273-289.

Uncapher, M.R., and Wagner, A.D. (2009). Posterior parietal cortex and episodic encoding: insights from fMRI subsequent memory effects and dual-attention theory. Neurobiol Learn Mem *91*, 139-154.

Utevsky, A.V., Smith, D.V., and Huettel, S.A. (2014). Precuneus is a functional core of the default-mode network. J Neurosci *34*, 932-940.

van Kesteren, M.T., Ruiter, D.J., Fernández, G., and Henson, R.N. (2012). How schema and novelty augment memory formation. Trends Neurosci *35*, 211-219.

Vilberg, K.L., and Rugg, M.D. (2008). Memory retrieval and the parietal cortex: a review of evidence from a dual-process perspective. Neuropsychologia *46*, 1787-1799.

Wagner, A.D., Schacter, D.L., Rotte, M., Koutstaal, W., Maril, A., Dale, A.M., Rosen, B.R., and Buckner, R.L. (1998). Building memories: remembering and forgetting of verbal experiences as predicted by brain activity. Science *281*, 1188-1191.

Wei, H., Jafarian, A., Zeidman, P., Litvak, V., Razi, A., Hu, D., and Friston, K.J. (2020). Bayesian fusion and multimodal DCM for EEG and fMRI. Neuroimage *211*, 116595.

Yang, Y., Zhong, N., Friston, K., Imamura, K., Lu, S., Li, M., Zhou, H., Wang, H., Li, K., and Hu, B. (2017). The functional architectures of addition and subtraction: Network discovery using fMRI and DCM. Hum Brain Mapp *38*, 3210-3225.

Yarkoni, T. (2009). Big Correlations in Little Studies: Inflated fMRI Correlations Reflect Low Statistical Power-Commentary on Vul et al. (2009). Perspect Psychol Sci *4*, 294-298.

Zeidman, P., Jafarian, A., Corbin, N., Seghier, M.L., Razi, A., Price, C.J., and Friston, K.J. (2019a). A guide to group effective connectivity analysis, part 1: First level analysis with DCM for fMRI. Neuroimage *200*, 174-190.

Zeidman, P., Jafarian, A., Seghier, M.L., Litvak, V., Cagnan, H., Price, C.J., and Friston, K.J. (2019b). A guide to group effective connectivity analysis, part 2: Second level analysis with PEB. Neuroimage *200*, 12-25.

Zweynert, S., Pade, J.P., Wüstenberg, T., Sterzer, P., Walter, H., Seidenbecher, C.I., Richardson-Klavehn, A., Düzel, E., and Schott, B.H. (2011). Motivational salience modulates hippocampal repetition suppression and functional connectivity in humans. Front Hum Neurosci *5*, 144.